Exp Oncol 2020
42, 3, 204–207

Experimental ONCOLOGY

BIOMAGNETISM OF TUMOR IN RATS WITH GUERIN'S CARCINOMA AFTER INJECTION OF FERROMAGNETIC NANOCOMPOSITE (FERROPLAT): CONTACTLESS MEASUREMENT

I.N. Todor[1], N.Yu. Lukianova[1,], M.A. Primin[2], I.V. Nedaywoda[2], V.F. Chekhun[1]*
[1]R.E. Kavetsky Institute of Experimental Pathology, Oncology and Radiobiology, National Academy of Sciences of Ukraine, Kyiv 03022, Ukraine.
[2]V.M. Glushkov Institute of Cybernetics, National Academy of Sciences of Ukraine, Kyiv 03187, Ukraine.

***Aim*: In order to develop fundamentally new technologies for non-invasive and safer diagnosis of cancer, we aimed to detect non-contact magnetic signals from a malignant tumor in animals treated or not-treated with the ferromagnetic nanocomposite Ferroplat. *Materials and Methods*: Guerin's carcinoma was used as a model of tumor growth. The biomagnetism of the tumor was evaluated in the dynamics of its growth. Ten days after tumor transplantation, Ferroplat was administered intravenously to half of the animals with the tumor and to half of the control animals. The magnitude of the magnetic signals was determined 1 h and every two days after administration of the nanocomposite using a Superconducting Quantum Interference Device magnetometer of the original design. *Results:* We have found that the magnetic signals coming from the tumor are significantly higher compared to control tumor-free animals. Intravenous administration of a ferromagnetic nanocomposite (Ferroplat: Fe_3O_4 + cisplatinum) led to a significant increase of the magnetic signal, especially in the tumor tissue, and inhibition of Guerin's carcinoma growth. Ferromagnetic nanoparticles (32.7 nm) are retained in malignant cells for a longer time than in normal ones. *Conclusion*: Tumor cells accumulate iron nanoparticles more intensively than normal ones. Nanocomposite Ferroplat can be used for a targeted delivery of cisplatin to malignant cells.**

***Key Words*: malignant tumor, ferromagnetic nanoparticles, cisplatinum, SQUID-magnetometry.**

DOI: 10.32471/exp-oncology.2312-8852.vol-42-no-3.14918

The magnetic field and magnetic susceptibility of a cell indicate its physiological state, and the study of these indices is of great importance for the development of new methods for both diagnosis and therapy of different diseases, in particular, cancer.

Highly sensitive Superconductive Quantum Interference Device (SQUID) magnetometers are often used to evaluate magnetic signals from the cell, organ, and the whole body [1–6]. Recently, SQUID sensors have been playing an important role in nanobiotechnology. The use of SQUID magnetometry and ferromagnetic nanoparticles allows to estimate their accumulation in the tumor and to cause hyperthermia in malignant tissue [7–12]. This is fundamentally important because tumor cells accumulate iron more intensely than normal ones [13–15]. Iron metabolism is also more intense in malignant cells [16–17]. Hence, the use of magnetic nanoparticles in oncology has a real prospect.

Given the above, we tried to estimate the magnetic signals coming from a malignant tumor. In order to develop fundamentally new technologies for non-invasive and safer diagnosis of the tumor process, the ferromagnetic nanocomposite Ferroplat was also used.

MATERIALS AND METHODS

***Experimental model*.** Female Wistar rats weighting 120–150 g bred in the vivarium of R.E. Kavetsky Institute of Experimental Pathology, Oncology and Radiobiology, NAS of Ukraine (Kyiv, Ukraine), were used. All experiments were carried out according to the rules of Ethic Committee.

The experimental animals were divided into two groups: control (tumor-free; n = 6) and animals with transplanted tumors (n = 10). As experimental model of malignant tumor, Guerin's carcinoma was chosen. Tumor transplantation was performed by subcutaneous injection of 20% Guerin's carcinoma cell suspension ($2.5 \cdot 10^6$ cells/rat) in the thigh area.

***Ferromagnetic nanocomposite*.** The nanocomposite Ferroplat (Fe_3O_4 + cisplatinum) was developed jointly with the scientists of the O.O. Chuiko Institute of Surface Chemistry, National Academy of Sciences of Ukraine under the leadership of Professor P.P. Gorbik. The magnetite was synthesized by the liquid-phase method [18]. The synthesized nanocomposite represents a monodispersion with a particle size of 32.7 nm. By atomic emission spectrometry, it was found that the concentration of Fe_3O_4 in the nanocomposite is 3 mg/ml, and the concentration of cisplatinum is 0.4 mg/ml. The ferromagnetic nanocomposite was injected into the animals once into the tail vein at a dose of 2 mg of cisplatin/kg of body weight.

***Design of experiment*.** Tumor biomagnetism was assessed in the dynamics of tumor growth. 10 days after tumor transplantation, half of the tumor-bearing animals (5 rats) and half of the control animals (3 rats) received single intravenous injection of Ferroplat. The magnitude of the magnetic signals of tumors was determined in 1 h after injection, and then every two days after the administration of the nanocomposite. During the measurement of the magnetic signal, each

*Correspondence: E-mail: nataluk10@gmail.com
Abbreviations used: SQUID – Superconductive Quantum Interference Device.
Submitted: July 22, 2020.

animal was anesthetized (Kalipsol, "Gedeon Richter", Hungary). An original SQUID magnetometer was used to evaluate the magnetic signal.

Non-contact SQUID magnetometry. Non-contact measurements of the parameters of the magnetic field in the air above the object under study were carried out using the SQUID-saseptometric system, developed and created at the V.M. Glushkov Institute of Cybernetics, NAS of Ukraine. The principle of operation of a magnetometric system is based on measuring the magnetic susceptibility of magnetic carriers that are inside an object (in our case, a rat). To measure the magnetic susceptibility, the antenna of the SQUID magnetometer is placed in the center of the Helmholtz coils, which create an alternating magnetic field (Fig. 1). By moving the object under investigation in the center of the magnetizing coils, the SQUID magnetometer registers a magnetic signal, the spatial distribution map of which is the basis for localizing magnetic carriers and evaluating their concentration. The magnetizing system consists of two mutually perpendicular pairs of coils on square frames with mutually perpendicular directions of the generated magnetic field (*Bx, By*). The measuring channel of the system is based on an axisymmetric SQUID gradient-meter of the second order d^2Bz/dz^2.

When performing the measurements, the dimensions of the grid above the object of research coincided with the boundaries of a square with a side of 60 mm in mutually perpendicular directions, and the number of measurement points was 36 (6x6 with a step of 12 mm) for a single-channel magnetometric system.

For the relative estimation of the level of the registered signal within the boundaries of the plane of the current object in relation to the "control" one, the signal estimate for each spatial map of the magnetic field distribution was calculated in the form:

$$E_m = \Sigma B_z^2$$

Here B_z is the magnitude of the output signal of the magnetometer (proportional to the component of the magnetic field of the object B_z), and the summation is carried out over all points of the measurement plane at which this value is known. For a correct comparison of graphical and numerical information, the found values of E_m (proportional to the energy of the magnetic field within the boundaries of the measurement area — energy characteristic) were normalized taking into account the number of points and matched in time.

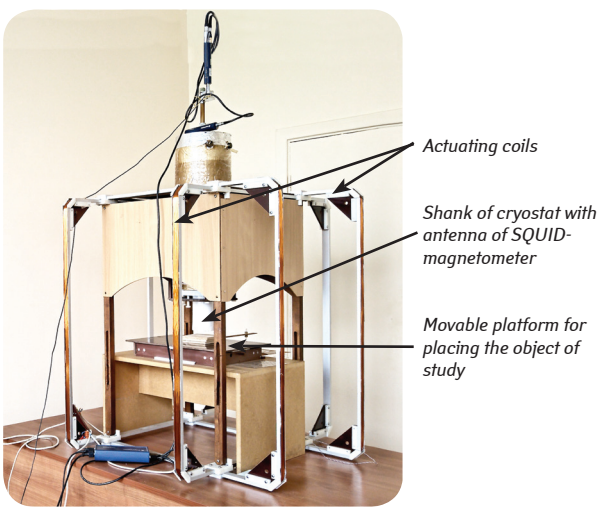

Fig. 1. Magnetometric system for experiments with small-size animals

Statistical processing of the data was performed using the software Statistica (v.7.0) and Student's *t*-test. The difference was considered statistically significant at $p < 0.05$.

RESULTS AND DISCUSSION

The study has revealed that the magnetic signal coming from the tumor (with a volume of 0.50 ± 0.05 cm^3) 6 days after its transplantation was slightly higher than that from the same area of the animal's body (back) in intact (control) rats. However, 8 days after the tumor transplantation, when the tumor increased in size, the magnetic signal coming from it was already significantly higher when compared with the control animals. Signal values recorded in Guerin's carcinoma in its growth dynamics are shown in Table 1 and Table 2. The maximum value of E_m of the magnetic signal and the value of the integral of the energy characteristic were as follows: 1.17 ± 0.08 a.u., 17.56 ± 1.57 a.u. for control animals and 1.82 ± 0.08 a.u., 27.57 ± 1.31 a.u. for animals with a tumor. The indicators obtained from tumor-bearing rats were 1.6 times higher than those of control animals. Note that the volume of the tumor was very small.

10 days after the tumor transplantation, its volume was 4.64 ± 0.73 cm^3. The tumor was at an exponential growth phase. The experimental animals were divided into subgroups. Three rats from the control group and five rats with Guerin's carcinoma were injected once into the tail vein with a ferromagnetic nanocomposite (Ferroplat) at a dose of 2 mg cisplatin/kg body weight. Exactly 1 h after the injection of Ferroplat, the magnitudes of the magnetic signals over the tumor of each animal were recorded using a SQUID magnetometer. Registration of magnetic signals was also carried out 12, 14, 16 and 18 days after tumor grafting.

As a result of research, we have found that in a tumor at the logarithmic phase of its growth, magnetic signals increase. This can be explained by the activation of iron consumption and its increased metabolism.

After Ferroplat injection, the magnetic signals increased significantly (see Table 1 and Table 2). Moreover, such effect was observed both in control tumor-free rats and in animals with a tumor. The maximum value of the E_m value of the magnetic signal in the tumor was 1.4 times higher than in the control ($p < 0.05$; see Table 1). At the same time, in Guerin's carcinoma, in comparison with the control, the integral values of magnetic signals were also 1.4 times higher ($p < 0.05$; see Table 2).

Subsequently (i.e., 12, 14, 16 and 18 days after tumor transplantation or 2, 4, 6, 8 days after Ferroplat administration), the intensity of the magnetic signal gradually decreased along with the growth of the tu-

Table 1. Maximum values of magnetic signals of the investigated objects (a.u.)

Group of rats	Days after tumor transplantation						
	6	8	10 (F)	12	14	16	18
Magnetic noise (before and after measurement session)	1.20 ± 0.25 (n = 4)	0.20 ± 0.19 (n = 4)	0.41 ± 0.20 (n = 4)	0.15 ± 0.04 (n = 4)	0.15 ± 0.08 (n = 4)	0.15 ± 0.10 (n = 4)	0.47 ± 0.01 (n = 4)
Control (tumor-free) animals	1.17 ± 0.19 (n = 6)	1.17 ± 0.08 (n = 6)	19.29 ± 1.51 (n = 3)	16.17 ± 4.26 (n = 3)	9.20 ± 2.40 (n = 3)	7.83 ± 0.36 (n = 3)	7.50 ± 2.10 (n = 3)
			0.33 ± 0.11 (n = 3)	0.55 ± 0.11 (n = 3)	0.65 ± 0.08 (n = 3)	1.27 ± 0.26 (n = 3)	0.53 ± 0.02 (n = 3)
Animals with Guerin's carcinoma (sensitive to cisplatin)	1.45 ± 0.13 (n = 10)	1.82 ± 0.08* (n = 10)	27.09 ± 1.18* (n = 5)	18.43 ± 3.18 (n = 5)	15.66 ± 2.16 (n = 5)	15.40 ± 1.38* (n = 5)	13.98 ± 1.70* (n = 5)
			1.60 ± 0.15* (n = 5)	1.85 ± 0.03* (n = 5)	1.80 ± 0.30* (n = 5)	1.86 ± 0.10* (n = 5)	1.42 ± 0.16* (n = 5)

Note: *$p < 0.05$ in comparison with control animals; (F) – Ferroplat intravenous injection.
Yellow background – animals treated with Ferroplat.

Table 2. Integral values of the magnetic signals of the investigated objects (a.u.)

Group of animals	Days after tumor transplantation						
	6	8	10 (F)	12	14	16	18
Magnetic noise (before the measurement session and after it)	17.57 ± 3.53 (n = 4)	2.73 ± 1.87 (n = 4)	6.11 ± 3.32 (n = 4)	2.11 ± 0.67 (n=4)	2.00 ± 1.15 (n=4)	2.31 ± 1.40 (n=4)	6.78 ± 0.19 (n=4)
Control (tumor-free) animals	16.69 ± 2.96 (n = 6)	17.56 ± 1.57 (n = 6)	298.39 ± 24.88 (n = 3)	252.14 ± 66.48 (n = 3)	140.27 ± 37.79 (n = 3)	122.14 ± 5.44 (n = 3)	114.03 ± 32.02 (n = 3)
			4.57 ± 1.78 (n = 3)	7.91 ± 1.54 (n = 3)	9.36 ± 1.11 (n = 3)	18.90 ± 3.87 (n = 3)	7.17 ± 0.33 (n = 3)
Animals with Guerin's carcinoma (sensitive to cisplatin)	20.90 ± 2.12 (n = 10)	27.57 ± 1.31* (n = 10)	423.56 ± 18.29* (n = 5)	289.85 ± 50.10 (n = 5)	245.65 ± 34.27 (n = 5)	242.02 ± 22.21* (n = 5)	216.49 ± 26.54* (n = 5)
			23.79 ± 2.52* (n = 5)	27.55 ± 0.34* (n = 5)	26.97 ± 4.86* (n = 5)	28.43 ± 1.56 (n = 5)	19.85 ± 2.48* (n = 5)

Note: *$p < 0.05$ in comparison with control animals; (F) – Ferroplat intravenous injection.
Yellow background – animals treated with Ferroplat.

mor. This was observed both in the control group and in the group of animals with tumor (see Table 1 and Table 2). However, the drop in the magnetic signal in rats with Guerin's carcinoma was less pronounced than in the control. These facts, apparently, represent further evidence that the metabolism of iron in tumor cells is more intensive than in normal cells. In addition, ferromagnetic nanoparticles are retained in malignant cells for a longer time. And given that Ferroplat contains a cytostatic (cisplatin), its increased accumulation in tumor cells due to ferromagnetic nanoparticles increases its antitumor effect and reduces side effects on the body.

All of the above, namely the enhancement of the magnetic signal recorded from the tumor after a single intravenous injection of Ferroplat, indicate that the ferromagnetic nanocomposite has penetrated into the cells of Guerin's carcinoma. The antitumor effect of Ferroplat was recorded. As can be seen from Fig. 2, the reduction in tumor volume under the influence of Ferroplat was 69% after 8 days after its administration ($p < 0.02$). This indicates the targeted delivery of the cytostatic agent (cisplatin, which is part of the nanocomposite) to tumor cells. The results obtained once again indicate the advisability of using ferromagnetic nanoparticles to increase the selectivity and effectiveness of cytostatic therapy.

We suppose that the scarcity of the data related to the administration of magnetic nanomaterials is one of the reasons that hinder their use as drug carriers. Additional research is needed on physical models of magnetic carriers with high specific magnetic

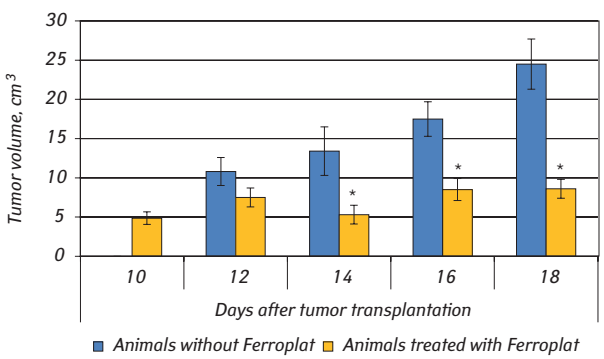

Fig. 2. The volume of Guerin's carcinoma after a single intravenous injection of Ferroplat. *$p < 0.05$ compared to the control

properties. At the same time, it is important to take into account their circulation time in the blood, the minimum nonspecific binding with cells (primarily immunocompetent ones), the possibility of immobilization of bioactive molecules on their surface, as well as the ability to controlled biodegradation. The size of nanoparticles in Ferroplat is approximately 32.7 nm, which ensured their rapid penetration into the cells. This is indicated by an increase in the magnetic signal.

In our experiments, a supersensitive SQUID-magnetometric system registers the spatial pattern of the distribution of magnetic carriers and, thus, drugs associated with them in the pathological zone. Special software makes it possible to reconstruct the picture and assess the dynamics of the distribution of magnetic carriers in the body. Such a system would be of importance for targeted cancer therapy providing the drug transport exclusively to the pathol-

ogy zone with monitoring of drug concentration in the targeted area for the required time. Our findings are in line with recent data on the prospective use of the magnetic nanoparticles in cancer therapy [19–22]. The preliminary data obtained in our study confirm that the use of SQUID magnetometry in cancer research has a real perspective and the nanocomposite Ferroplat could be used for the targeted delivery of cisplatin to malignant cells.

ACKNOWLEDGMENT

The work was carried out within the framework of the integrated target program for fundamental research of the National Academy of Sciences of Ukraine "Fundamental problems of development of new nanomaterials and nanotechnologies", 2015–2019.

REFERENCES

1. **Hathaway HJ, Butler KS, Adolphi NL**, ***et al.*** Detection of breast cancer cells using targeted magnetic nanoparticles and ultra-sensitive magnetic field sensors. Breast Cancer Res 2011; **13**: R108.

2. **Yao L, Xu S.** Detection of magnetic nanomaterials in molecular imaging and diagnosis applications. Nanotechnol Rev 2014; **3**: 247–68.

3. **De Haro LP, Karaulanov T, Vreeland EC, *et al.*** Magnetic relaxometry as applied to sensitive cancer detection and localization. Biomed Tech (Berl) 2015; **60**: 445–55.

4. **Körber R, Storm J-H, Seton H, *et al***. SQUIDs in biomagnetism: a roadmap towards improved healthcare. Supercond Sci Technol 2016: **29**: 1–30.

5. **Huang MX, Anderson B, Huang CW, *et al.*** Development of advanced signal processing and source imaging methods for superparamagnetic relaxometry. Phys Mol Biol 2017; **62**: 734–57.

6. **Clarke J, Lee Y-H, Schneiderman J**. Focus on SQUIDs in Biomagnetism. Superconductor Sci Tech 2018; **31**: 1–7.

7. **Richter H, Kettering M, Wiekhorst F, *et al.*** Magnetorelaxometry for localization and quantification of magnetic nanoparticles for thermal ablation studies. Phys Med Biol 2010; **55**: 623–33.

8. **Liebl M, Wiekhorst F, Eberbeck D, *et al.*** Magnetorelaxometry procedures for quantitative imaging and characterization of magnetic nanoparticles in biomedical applications. Biomed Tech (Berl) 2015; **60**: 427–43.

9. **Chieh JJ, Huang KW, Lee YY, *et al***. Dual-imaging model of SQUID biosusceptometry for locating tumors targeted using magnetic nanoparticles. J Nanobiotechnology. **13**:11. doi: 10.1186/s12951-015-0069-5.

10. **Arriortua OK, Garaio E, Herrero de la Parte B, *et al.*** Antitumor magnetic hyperthermia induced by RGD-functionalized Fe_3O_4 nanoparticles, in an experimental model of colorectal liver metastases. J Nanotechnol 2016; **7**: 1532–42.

11. **Chang D, Lim M, Goos JACM, *et al.*** Biologically targeted magnetic hyperthermia: potential and limitations. Front Pharmacol 2018; **9**: 831. doi: 10.3389/fphar.2018.00831.

12. **Balejcikova L, Molcan M, Kovac J, *et al.*** Hyperthermic effect in magnetoferritin aqueous colloidal solution. J Mol Liq 2019; **283**: 39–44.

13. **Toyokuni S**. Role of iron in cancerogenesis: Cancer as a ferrotoxic disease. Cancer Sci 2009; **100**: 9–16.

14. **Anderson GJ, McLaren GD**. Iron Physiology and Pathophysiology in Humans. Springer Science & Business Media, 2012: 703 p.

15. **Lamy PJ, Durigova A, Jacot W**. Iron homeostasis and anemia markers in early breast cancer. Clin Chim Acta 2014; **434**: 434–40.

16. **Torti SV, Torti FM**. Iron and cancer: more ore to be mined. Natl Rev Cancer 2013; **13**: 342–55.

17. **Torti SV, Torti FM**. Cellular iron metabolism in prognosis and therapy of breast cancer. Crit Rev Oncog 2013; **18**: 435–48.

18. **Gorbyk PP, Chekhun VF.** Nanocomposites of medicobiologic destination: reality and perspectives for oncology. Functional materials 2012; **19**: 145–56.

19. **Hosu O, Tertis M, Cristea C.** Implication of magnetic nanoparticles in cancer detection, screening and treatment. Magnetochemistry 2019; **5**, 55; doi:10.3390/magnetochemistry5040055.

20. **Jabalera Y, Garcia-Pinel B, Ortiz R, *et al.*** Oxaliplatin-biomimetic magnetic nanoparticle assemblies for colon cancer-targeted chemotherapy: an in vitro study. Pharmaceutics 2019; **11**, 395; doi:10.3390/pharmaceutics11080395.

21. **Nogueira J, Soares SF, Amorim CO, *et al.*** Magnetic driven nanocarriers for pH-responsive doxorubicin release in cancer therapy. Molecules 2020; **25,** 333; doi:10.3390/molecules25020333.

22. **Ferreira M, Sousa J, Pais A, *et al.*** The role of magnetic nanoparticles in cancer nanotheranostics. Materials 2020; **13**, 266; doi:10.3390/ma13020266.